THE ASTROPHYSICAL JOURNAL, 576:L49–L52, 2002 September 1
© 2002. The American Astronomical Society. All rights reserved. Printed in U.S.A.

WHY IS IT DIFFICULT TO DETECT A MILLISECOND PULSAR IN NEUTRON STAR X-RAY BINARIES?

LEV TITARCHUK,[1,2] WEI CUI,[3] AND KENT WOOD[2]

Received 2002 May 7; accepted 2002 July 24; published 2002 August 1

ABSTRACT

We explain why it is possible to detect directly X-ray emission from near the surface of the neutron star (NS) in SAX J1808.4−3658 but not in most other low-mass X-ray binaries (LMXBs), with the exception that emission from the surface can be seen during burst events. We show that the X-ray emission from SAX J1808.4−3658 mostly originates in the Comptonization process in a relatively optically thin hot region (with an optical depth τ_0 around 4 and temperature around 20 keV). Such a transparent region does not prevent us from detecting coherent X-ray pulsation due to hot spots on the NS surface. We give a precise model for the loss of modulation: such suppression of the quasi-periodic oscillation (QPO) amplitude due to scattering can explain the disappearance of kilohertz QPOs with increasing QPO frequency. We also formulate general conditions under which the millisecond X-ray pulsation can be detected in LMXBs. We demonstrate that the observed soft phase lag of the pulsed emission is a result of the downscattering of the hard X-ray photons in the relatively cold material near the NS surface. In the framework of this downscattering model, we propose a method to determine the atmosphere density in that region from soft-lag measurements.

Subject headings: accretion, accretion disks — pulsars: individual (SAX J1808.4−3658) — stars: neutron — X-rays: stars

1. INTRODUCTION

Low-mass X-ray binaries (LMXBs) presumably contain a weakly magnetized neutron star (NS). Recently, Titarchuk, Bradshaw, & Wood (2001, hereafter TBW) suggested a new method of estimating *B*-field strength using the magnetoacoustic oscillation model and found that the *B*-field strength for a number of NSs in LMXBs is $\sim 10^8$ G. Near-coherent millisecond X-ray pulsations have been observed in 4U 1728−34 during thermonuclear (type I) X-ray bursts (e.g., Strohmayer et al. 1996). They are interpreted as X-ray intensity modulated at a period close to the spin period of the NS. Thus, these *B*-field estimates in addition to the detection of the millisecond pulsation give strong arguments for LMXB NSs to be progenitors of millisecond radio pulsars (MLPs; see review by Bhattacharya & van den Heuvel 1991). But there is still a question of why these coherent pulsations are not found in persistent emission despite careful searches (Wood et al. 1991; Vaughan et al. 1994; Chandler & Rutledge 2000). The lack of coherent pulsations has been explained as modulation loss from gravitational lensing (Wood, Ftaclas, & Kearney 1988; Mészáros, Riffert, & Berthiaume 1988) or from to scattering (e.g., Bainerd & Lamb 1987; Kylafis & Klimmis 1987). The third explanation for the lack of pulsations is presented by Cumming, Zweibel, & Bildsten (2001), who argue that the surface field is weak because of magnetic screening.[4] In this Letter, we put forth arguments for the smearing out of the pulsar signal due to electron scattering in the optically thick environment typical of most observed LMXBs. In § 2, we study the scattering effect and its relation with the observed timing and spectral characteristics for various quasi-periodic oscillation (QPO) sources. In § 3, we investigate the scattering effects in QPO sources. In § 4, we present results of the *Rossi X-Ray Timing Explorer* (*RXTE*) data analysis of spectral properties of X-radiation in SAX 1808.4−3656. In § 5, we analyze the downscattering model and its application to the observed soft-lag phenomenon detected in the coherent pulse signal from SAX 1808.4−3656. Conclusions follow in § 6.

2. SCATTERING EFFECT ON THE QPO PULSE PROFILE AND PULSAR PROFILE

The transfer problem to be solved is that of a sinusoid, representing either (1) an intrinsic pulsar light curve or (2) a high-frequency QPO, but in each case seen through a surrounding medium that reduces the pulse modulation by scattering (see Fig. 1 for a schematic picture of the model geometry). The signal whose modulation is affected lies in the range of a few hundred hertz to perhaps 1 kHz. We thus must analyze the smearing out of a signal at very high frequencies and investigate the dependence on both the intrinsic frequency and the optical depth of the scattering environment. The geometry used derives from earlier works (see, e.g., Sunyaev & Titarchuk 1980, hereafter ST80; Titarchuk, Lapidus, & Muslimov 1998, hereafter TLM98) modeling energy spectra and power density spectra (PDS) of LMXB sources. *For the high-frequency QPO* (*case 1*)*, the TLM98 model identifies the site where the QPO is generated*, which will be at a radius substantially larger than that of the star. Thus, the effective optical depth of interest in case 2 will not be the full optical depth to the star surface but rather the reduced optical depth appropriate to that site location.

The total change in QPO power as the source varies will be a combination of two effects, namely, (1) the intrinsic change in QPO power that results simply from the physics of shifting the resonance frequency that gives the QPO and (2) the further reduction in power that results from its now being *observed at higher frequency and through greater optical depth*, both of which enhance the effects of scattering. To model the entire process, we therefore require a model for the intrinsic change

[1] Center for Earth Observing and Space Research, George Mason University, Fairfax, VA 22030-4444.

[2] US Naval Research Laboratory, Space Science Division, 4555 Overlook Avenue, SW, Washington, DC 20375-5352; lev@xip.nrl.navy.mil; kwood@ssd5.nrl.navy.mil.

[3] Department of Physics, Purdue University, 1396 Physics Building, West Lafayette, IN 47907; cui@physics.purdue.edu.

[4] The recent discoveries of MLPs in XTE J1751−305 (Markwardt et al. 2002) and in XTE J0929−314 (Galloway et al. 2002) with extremely low mass transfer rates support the suggestion of the absence of the magnetic screening for the low mass accretion rates.

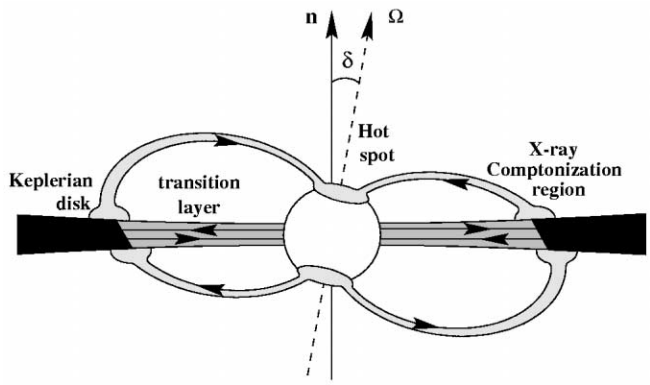

FIG. 1.—Schematic picture of the model geometry SAX J1808.4−3658. The hot flow forming at the outer boundary of the transition layer streams toward the NS along magnetic field lines. The reflection of the hard radiation of the flow from the NS surface results in soft time lags of the pulsed emission.

in power. This is provided in the cited transition layer (TL) model (TLM98) by approximating the QPO process itself as a damped harmonic oscillator under the influence of a driving force. Then, the interaction leads to resonance oscillations for which the Q-value ($\nu_{\rm QPO}/\delta\nu_{\rm QPO}$) can be high. The resonance amplitude varies as the product of the amplitude of the driving force $A_{\rm dr}(\nu)$ and $1/\nu_{\rm QPO}$ (see Landau & Lifshitz 1965). The default intrinsic model, in the absence of scattering, is thus that the QPO amplitude falls off as $A(\nu) = A_{\rm dr}(\nu)/\nu_{\rm QPO}$, but scattering contributes additional reduction. In a source such as GX 340+0, where a *pair* of high-frequency QPOs is seen, it is possible to test these ideas in detail, using the model derived below and applying it to both QPOs, keeping the optical depth τ_0 the same for both kilohertz QPOs because they are colocated. Detection of the NS spin period is the crucial further issue at stake here. The typical problem is the following: since the NS spin gives a *coherent* periodic signal at nearly constant frequency, it should be at a relative *advantage* in detectability in comparison with QPOs, yet it is not seen while the QPOs *are* seen. The key, obviously, is that the QPO sees the reduced optical depth while the modulation at the spin period experiences the unreduced optical depth. The occasional exceptions where the stellar spin frequency does prove detectable (such as MLPs, plus the transient detections in X-ray bursters) should be explicable in terms of circumstances that reduce scattering effects in those particular cases below values that are generally obtained; moreover, those exceptional reductions should be confirmed by spectra indicative of the lower optical depth and other supporting context observations.

For a quantitative model of this problem, scattering is handled as a diffusion problem in Green's function [$G(t)$] treatment. The input pulse is $x(t) = A\sin(\omega t + \varphi_0)$, where $\omega = 2\pi\nu$ is the NS spin rotational frequency ω or the QPO centroid frequency, depending on whether it is case 1 or 2, and φ_0 is an initial phase. The resulting pulse affected by the scattering is $z(t)$ and is given by a convolution of $x(t)$ and $G(t)$:

$$z(t) = \int_0^t x(t')G(t-t')dt'. \quad (1)$$

For times t much greater than the scattering time in the Compton cloud $R\tau/c$ and the initial pulse emission $x(t) = A(\omega)\exp[(\omega t + \varphi_0)i]$, the resulting pulse is calculated as follows:

$$z(t) = A(\omega)\exp[i(\omega t + \varphi_0)]I(\omega),$$

$$I(\omega) = \int_0^\infty e^{-i\omega u}G(u)du. \quad (2)$$

ST80 analyzed the response of the scattering medium (the Green function) for various source distributions. They show that for a QPO source embedded in the center of the cloud ($\tau = 0$), the response of the scattering medium (the Green function), $G(t)$, can be approximated by

$$G(t) \propto (C_1 + C_2 t^{-5/2}) \times \exp\left[-3R\tau_0/4ct - \pi^2 c\tau_0 t/3R\left(\tau_0 + \frac{2}{3}\right)^2\right], \quad (3)$$

where τ_0 and R are optical depth and radius of the cloud, respectively, and c is the light speed. Coefficients C_1 and C_2 can be estimated as follows (see also Wood et al. 2001): $C_1 = 5\pi^2/3(\tau_0 + \frac{2}{3})^2$, and $C_2 = \pi(3/\pi)^{3/2}\tau_0^{1/2}(R/c)^{5/2}/4$. Using equation (3), the integral $I(\omega)$ is analytically calculated by the steepest descent method (see also Prudnikov, Bruchkov, & Marichev 1981, eq. [2.3.16]). We can show that an amplitude $B(\omega)$ of $z(t)$ can be obtained as

$$B(\omega) = A(\omega)\mathcal{F}(\mathcal{X})\exp(-2\mathcal{X}), \quad (4)$$

where $\mathcal{X}(\omega, \tau_0) = \{[\pi\tau_0/2(\tau_0 + \frac{2}{3})]^4 + (3R\tau_0\omega/4c)^2\}^{1/2}$ and $\mathcal{F}(\mathcal{X}) = d_1\mathcal{X}^{1/2} + d_2\mathcal{X}^{-3/4} + d_0$ is a weak function of $\mathcal{X}$, which is a constant, and the product of $\mathcal{F}(\mathcal{X})\exp(-2\mathcal{X})$ is almost unity for ω much less than the inverse of crossing time $t_0^{-1} = (R\tau_0/c)^{-1}$. The amplitude $B(\omega)$ decays exponentially when ω increases.

3. CONSEQUENCES OF SCATTERING EFFECTS FOR QPO OBSERVATIONS: EVIDENCE OF THE RESONANCE EXCITATION IN THE QPO SOURCES

As seen from equation (4), the amplitude of the NS pulsations with $\omega \sim 2\pi \times 400$ Hz decreases very rapidly with τ_0 for

$$\tau_0 \gtrsim 4[(c/R)/5 \times 10^3\ {\rm s}^{-1}]/[\omega/(2\pi \times 400\ {\rm Hz})]. \quad (5)$$

A radius R of 60 km was chosen as a typical radius of the Compton cloud derived from the observations in the framework of the TL model (see TBW). In Figure 2, we present the rms amplitude of the high-frequency QPOs as a function of kilohertz frequencies for the Z source GX 340+0 using the results of Jonker et al. (2000). We compare them with the theoretical model presented by equation (4). The amplitude of the lower kilohertz QPOs is perfectly fitted by $1/\omega$ dependence (see the dashed line on the left-hand side of Fig. 2); $\chi^2_{\rm red} = 0.53$ for this fit, but the deviation of $B(\omega)$ due to scattering (the solid line on the right-hand side of Fig. 2) from the $1/\omega$ law (the dashed line on the right-hand side of Fig. 2) is clearly seen for the higher kilohertz QPOs. The best fit to the data ($\chi^2_{\rm red} = 1.1$) by equation (4) with $A(\omega) \propto 1/\omega$ is obtained for $\tau_0 = 2.7$, with $R/c = 10^{-4}$ s. For $\tau_0 = 2.7$, the rms, $B(\omega)$ calculated for low kilohertz frequencies is almost identical to $1/\omega$ dependence ($\chi^2_{\rm red} = 0.85$). Thus, we find that the driving force amplitude $A_{\rm dr}$ is practically independent of frequency for kilohertz QPOs. One can argue that the

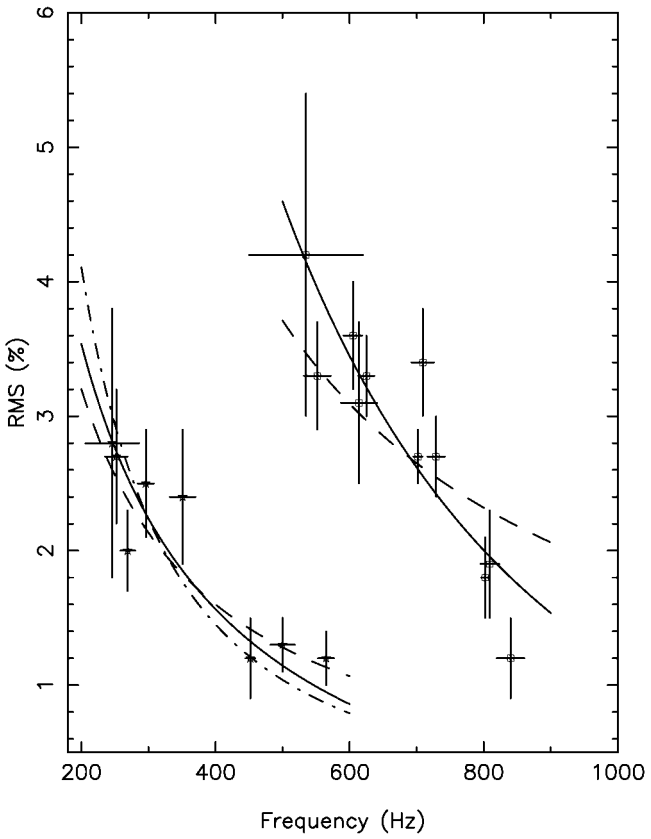

FIG. 2.—Examples of rms amplitude vs. QPO frequency for lower and higher kilohertz peaks for GX 340+0 (Jonker et al. 2000). The two solid lines (for lower and higher peaks, respectively) are theoretical curves for which scattering effects are taken into account. The dashed lines are for the $1/\nu$ law, and the dash-dotted line is for the $\nu^{-3/2}$ law.

driving force power for kilohertz QPOs can be determined by the observed PDS at kilohertz frequencies. The PDS power-law index β typically varies around 1 (see details in Wijnands & van der Klis 1998). The resulting resonance amplitude would be $\omega^{-(1+\beta/2)}$ with an assumption that this power continuum is a driving force reservoir for the resonance. As an example, we fit this $\omega^{-(1+\beta/2)}$ model with $\beta = 1$ to the data for the *lower* kilohertz QPOs only, where the scattering effects can be neglected (see inequality [5]). We find that for this model $\chi^2_{\rm red} = 1.37$. The rms-frequency dependence for the lower kilohertz QPOs is not affected by scattering; it affects mainly the higher kilohertz QPOs (see eq. [5]). The scattering effects make the rms-frequency dependence much steeper for the higher kilohertz QPOs, which does not allow us to extract the true driving force amplitude from the data (clearly, it is not feasible to dispense with scattering and fit both QPOs solely with a type of driving force model).[5] In § 4, we show that in SAX J1808.4−3658 the optical depth of the spherical Compton cloud is relatively low, allowing detections.

4. X-RAY SPECTRA OF SAX J1808.4−3658 AND OF OTHER LMXBs

We revisit some *RXTE* spectral data for SAX J1808.4−3658 (Gilfanov et al. 1998; Heindl & Smith 1998). The spectrum (which was constructed using data from 30411-01-06-00) is well represented by the Comptonization model (CompTT in XSPEC, with spherical geometry; Titarchuk 1994) along with some contribution from a blackbody component and an Fe Kα line. The best-fit parameters of the model are $\tau_0 = 4.5^{+0.55}_{-0.97}$, electron temperature $kT_e = 19.5^{+7.8}_{-3.2}$ keV, and Kα energy 6.5 ± 0.1 keV. The temperature of the seed photons for the Comptonization is within $kT_0 = 0.1^{+0.4}_{-0.1}$ keV. The temperature of the blackbody radiation (presumably from the NS surface) is $kT_{\rm bb} = 0.69 \pm 0.02$ keV. The quality of the fit is high, with $\chi^2 = 294/322 = 0.91$.[6] It is worth noting the relatively small optical depth $\tau = 4.5$. This can be the main reason why the NS pulsation is detected from this source (see inequality [5]). If this τ_0 is compared with that for other LMXB sources (showing QPO features), one finds that optical depths for a number of sources are higher than that for SAX J1808.4−3658. They are 10–11 for Cyg X-2 (Kuznetsov 2002), Sco X-1, and GX 340+0, and τ_0 is around 6 for 4U 1728−34 (TBW). On average, the seed photon temperature value $T_0 \ll T_{\rm bb}$. Presumably, the photon supply for Comptonization mostly comes from the relatively cold disk and the blackbody emission comes from the NS surface. The Comptonization spectra of the QPO sources where the NS pulsations are not observed is indirect evidence for this. Van der Klis (2000) argues that there is a striking similarity between the power spectra of black holes, atoll sources, Z sources and the MLP SAX J1808.4−3658. This would exclude any spectral formation models requiring a material surface and would essentially imply that the phenomena are generated in the accretion disk around any low magnetic field compact object. But in the case of SAX J1808.4−3658 we definitely see coherent pulsations of the hard radiation that originates in the NS surface (Cui, Morgan, & Titarchuk 1998, hereafter CMT98), and we should also see the downscattering effect of the hard Comptonized photons when they hit the relatively cold material of the NS star (see Fig. 3).

5. DOWNSCATTERING EFFECT

For SAX J1808.4−3658, the observed characteristics of the pulsed X-ray emission (pulse profiles and phase lags) and the overall energy spectrum provide useful insight into X-ray production processes and the emission environment. Important information regarding the density of the NS atmosphere can be extracted from the time lags between different energy bands. The soft lags have been detected for SAX J1808.4−3658 by CMT98.[7] The soft phase lag can be due to reflection (Compton downscattering) of the pulsed hard radiation from the NS atmosphere. In fact, this effect is unavoidable when hot plasma streams converge toward the NS magnetic poles. The hard radiation at the pole illuminates adjoining regions where a significant fraction of the hard radiation is reflected. For simplicity, we assume the input hard photons are monochromatic with energy E_h. The photons that emerge from the NS atmosphere with lower energy E_l arrive at a distant observer later than

[5] Fits of the rms amplitude vs. frequency similar to that presented in Fig. 2 for GX 340+0 have been produced for GX 5-1, Cyg X-2, GX 17-2, and Sco X-1. Thus, one can conclude that in all these kilohertz QPO observations the rms resonance amplitude $1/\omega$ vs. frequency is affected by the photon scattering.

[6] Gierliński, Done, & Barret (2002, hereafter GDB) also analyzed the X-ray spectrum of SAX J1808.4−3658, and they showed the spectrum can be fitted by a three-component model (blackbody component, Comptonization component, and Compton reflection). In general, spectral modeling is not unique, and it is not by chance that our spectral model and global picture are different from that of GDB. Because at $kT_{\rm bb}$ around 0.7 keV the iron is highly ionized, we conclude that the observed Kα (see § 4 and GDB) is formed as a result of the disk reflection rather than as the NS reflection.

[7] Galloway et al. (2002) also found the hard X-ray pulses arrived up to 770 μs earlier than the soft X-ray pulses in XTE J0929−314.

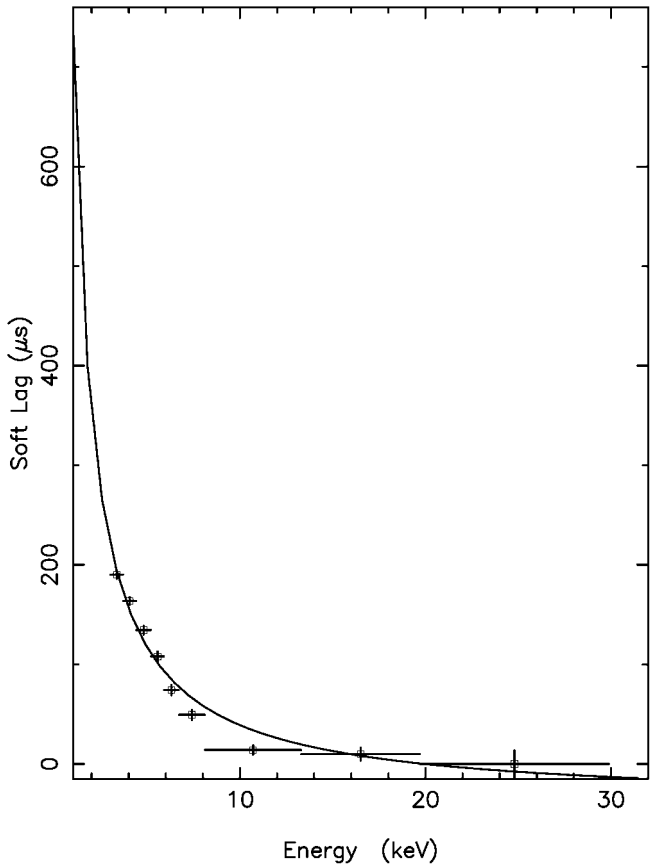

FIG. 3.—Measured soft X-ray lags with respect to the 20–30 keV band along with the best-fit downscattering model.

those with higher energy E_h. *The delay in arrival time, δt, is given by ul/c, where u is the number of scatterings undergone by the seed hard photon with energy* E_h before emerging with energy E_l, and $l = 1/n_e\sigma_T$ is the Thomson mean free path for the photon. The average fractional energy loss for the photon of energy E after each scattering is nearly independent of T_{bb}, and it is given by $\delta E/E \approx -(E - 4kT_{bb})/m_ec^2 \approx -E/m_ec^2$ (because $4kT_{bb} \ll E$), where m_ec^2 is the electron rest mass. Integrating over multiple scatterings, we have $u = m_ec^2(1/E_l - 1/E_h)$ (ST80). The measured soft lag scales as E^{-1}, as shown in Figure 3, and levels off above 10 keV. In Figure 3, we also show the best fit to the data using the downscattering model:

$$E^{-1} = E_h^{-1} + D\delta t. \quad (6)$$

We fit the theoretical E^{-1} as a function of δt to the measured quantities. The best-fit parameters are $E_h = 20$ keV and $D = 1.3 \times 10^{-3}$ μs^{-1} keV^{-1}, for which $\chi^2_{red} = 11.3/9 = 1.2$. Because $D = n_e c\sigma_T/m_ec^2$, we find that *the NS density near the surface is* $n_e = Dm_ec^2/c\sigma_T = 3.3 \times 10^{19}$ cm^{-3}. The measured soft lags in the frameworks of the downscattering models allow us to estimate the optical depth τ up to what the hard photon can penetrate illuminating the NS atmosphere. It takes more than 70 scatterings for 20 keV photons to reach the 5 keV energy band. As is known from the diffusion theory (see, e.g., ST80), a photon in the course of the random diffusion propagation to optical depth τ undergoes on average $N_{sc} \sim \tau^2$ scatterings. Thus, using $N_{sc} = 70$ (the scattering number of the input photons that finally emerge), one can deduce the penetration optical depth $\tau_{pr} = (N_{sc}/2)^{1/2} = 6$. In other words, the thickness of the NS reflection slab is approximately $(m_p/\sigma_T)\tau_{pr} = 15$ g cm^{-2}. Photoelectric absorption is suppressed at $kT_{bb} = 0.7$ keV, and thus one can estimate τ_{pr} neglecting the photoelectric extinction. The deduced τ_{pr} leads to an estimate of the reflection albedo of $A = 1 - (3\tau_{pr}/4 + 1)^{-1} = 0.82$ (see, e.g., Sobolev 1975). It means that more than 80% of the input hard photons are reflected by the NS atmosphere.

6. CONCLUSIONS

Our analysis of the timing and spectral properties of the millisecond pulsar SAX J1808.4−3658 and comparison of them with those for LMXB QPO sources leads us to these conclusions: (1) The detection of the NS pulsations from SAX J1808.4−3658 was possible because of the relatively transparent Compton cloud covering in this source ($\tau_0 \sim 4$). For the majority of the analyzed LMXBs, the Compton cloud optical depth is at least twice as high as that in SAX J1808.4−3658. The high-frequency pulsations with frequencies $\gtrsim$300 Hz are strongly wiped out by scattering in the clouds with $\tau_0 > 4$. SAX J1808.4−3658 is a limiting case for this detection. There is a possibility of finding the NS pulsations in the sources that are much less luminous (than these bright QPO LMXBs), because in them the Compton cloud is more transparent ($\tau_0 \lesssim 4$) for the NS pulsed radiation. (2) The rms amplitude of the kilohertz QPOs versus frequency follows the resonance law $1/\omega$ and is weakened by scattering in the Compton cloud. (3) The soft-lag measurements along with the implementation of the downscattering model can provide a tool for density determination near the NS surface.

We appreciate the fruitful discussions with P. Ray, S. Kuznetsov, and, particularly, with the referee.

REFERENCES

Bhattacharya, D., & van den Heuvel, E. P. J. 1991, Phys. Rep., 203, 1
Brainerd, C. B., & Lamb, F. K. 1987, ApJ, 317, L33
Chandler, A. M., & Rutledge, R. E. 2000, ApJ, 545, 1000
Cui, W., Morgan, E. H., & Titarchuk, L. G. 1998, ApJ, 504, L27 (CMT98)
Cumming, A., Zweibel, E., & Bildsten, L. 2001, ApJ, 557, 958
Galloway, D. K., et al. 2002, ApJL, submitted (astro-ph/0206493)
Gierliński, M., Done, C., & Barret, D. 2002, MNRAS, 331, 141 (GDB)
Gilfanov, M., Revnivtsev, M., Sunyaev, R., & Churazov, E. 1998, A&A, 338, L83
Heindl, M., & Smith, D. M. 1998, ApJ, 506, L35
Jonker, P. G., et al. 2000, ApJ, 537, 374
Kuznetsov, S. 2002, Astron. Lett., 28, 73
Kylafis, N. D., & Klimmis, G. S. 1987, ApJ, 323, 678
Landau, L. D., & Lifshitz, E. M. 1971, Mechanics (New York: Pergamon)
Markwardt, C. B., et al. 2002, ApJ, 575, L21
Mészáros, P., Riffert, H., & Berthiaume, G. 1988, ApJ, 325, 204
Prudnikov, A. P., Bruchkov, Yu. A., & Marichev, O. I. 1981, Integrals and Series (Moscow: Nauka)
Sobolev, V. V. 1975, Light Scattering in Atmospheres (Oxford: Pergamon)
Strohmayer, T. E., et al. 1996, ApJ, 469, L9
Sunyaev, R., & Titarchuk, L. G. 1980, A&A, 86, 121 (ST80)
Titarchuk, L. G. 1994, ApJ, 434, 570
Titarchuk, L. G., Bradshaw, C. F., & Wood, K. S. 2001, ApJ, 560, L55 (TBW)
Titarchuk, L. G., Lapidus, I., & Muslimov, A. 1998, ApJ, 499, 315 (TLM98)
van der Klis, M. 2000, ARA&A, 38, 717
Vaughan, B. A., et al. 1994, ApJ, 435, 362
Wijnands, R., & van der Klis, M. 1998, ApJ, 507, L63
Wood, K. S., Ftaclas, C., & Kearney, M. 1988, ApJ, 324, L63
Wood, K. S., et al. 1991, ApJ, 379, 295
———. 2001, ApJ, 563, 246